



# NASA CONTRACTOR REPORT

NASA CR-38

a.1

NASA CR-389

LOAN COPY: RETURN TO  
AFWL (WLIL-2)  
WRIGHT AFB, N MEX

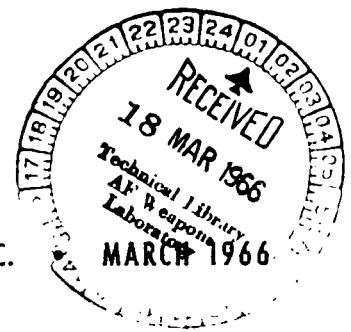
## RADIATION-RESISTANT DEVICE PHENOMENA

*by William C. Follmer and James P. Spratt*

Prepared under Contract No. NASw-997 by  
PHILCO CORPORATION  
Blue Bell, Pa.

for

NATIONAL AERONAUTICS AND SPACE ADMINISTRATION • WASHINGTON, D. C.





RADIATION-RESISTANT DEVICE PHENOMENA

By William C. Follmer and James P. Spratt

Distribution of this report is provided in the interest of information exchange. Responsibility for the contents resides in the author or organization that prepared it.

Prepared under Contract No. NASw-997 by  
PHILCO CORPORATION  
Blue Bell, Pa.

for

NATIONAL AERONAUTICS AND SPACE ADMINISTRATION

---

For sale by the Clearinghouse for Federal Scientific and Technical Information  
Springfield, Virginia 22151 - Price \$2.00

## ABSTRACT

Experimental studies of the mean-free-path of energetic electrons in metal films and the properties of reactively evaporated aluminum-oxide films are described in this report.

The energetic electron mean-free-path experiment has been carefully evaluated. Because of the extreme experimental difficulties encountered, and also because of the limited usefulness of the results in the light of the theoretical predictions regarding the input-to-output current transport efficiencies of a hot-carrier device, this experiment has been terminated.

The properties of reactively evaporated aluminum-oxide films have been studied as a function of the oxygen pressure, deposition rate, and thickness of the film. It has been determined experimentally that an oxide protective layer practically eliminates the sensitivity of the devices to atmospheric exposure. Insulating and semi-insulating films have been prepared. The semi-insulating films show a small photosensitivity.

## TABLE OF CONTENTS

Section	Page
SUMMARY . . . . .	1
Aluminum-Oxide Films . . . . .	1
Energetic Electron Transport . . . . .	1
INTRODUCTION . . . . .	2
Aluminum-Oxide Films . . . . .	2
Energetic Electron Transport . . . . .	3
ALUMINUM-OXIDE FILMS . . . . .	4
Device Fabrication . . . . .	4
Bulk Material Analysis . . . . .	4
Electron microscope test . . . . .	4
X-ray diffraction . . . . .	6
Electron-induced fluorescence . . . . .	6
Spectrographic analysis of aluminum films . . . . .	6
Thickness measurements . . . . .	6
Electronic Device Evaluation . . . . .	8
Effects of varying O <sub>2</sub> pressures . . . . .	8
Effects of ambient gas . . . . .	13
Film contamination . . . . .	14
DC I-V characteristics . . . . .	20
Conclusions . . . . .	21
ELECTRON TRANSPORT THROUGH THIN FILMS . . . . .	22
Transport Experiment . . . . .	22
Conclusions . . . . .	23
OVERALL CONCLUSIONS . . . . .	24
Aluminum-Oxide Films . . . . .	24
Energetic Electron Transport . . . . .	24

## LIST OF ILLUSTRATIONS

Figure		Page
1	Electron Micrograph of Oxide Film (Dark Area), Magnification = 80,000X . . . . .	5
2	Electron Diffraction Pattern of Oxide Film . . . . .	5
3	C/A Versus O <sub>2</sub> Pressure . . . . .	9
4	Dissipation Factor Versus O <sub>2</sub> Pressure . . . . .	10
5	$\rho_f \epsilon_r$ Versus O <sub>2</sub> Pressure . . . . .	11
6	$r_{ac}$ Versus O <sub>2</sub> Pressure . . . . .	12
7	Capacity Versus Time . . . . .	15
8	$r_{ac}$ Versus Time . . . . .	16
9	Dissipation Factor Versus Frequency . . . . .	18
10	Capacitance Versus Frequency . . . . .	19

## SUMMARY

### Aluminum-Oxide Films

Numerous aluminum-oxide samples have been fabricated with varying deposition rate and oxygen pressure. The effect of this systematic variation has been determined by admittance measurements as a function of frequency from dc to 1 megacycle. Initial thickness measurements have indicated that the density is considerably less than bulk aluminum oxide. Over the frequency range from  $10^3$  to  $10^6$  cps, the dissipation factor of insulating films is typically 0.01 or less.

Semi-insulating films have been prepared by reducing the oxygen pressure below  $6 \times 10^{-5}$  mmHg. A systematic increase in dissipation factor and capacitance occurred as the oxygen pressure was reduced to below  $6 \times 10^{-5}$  mm Hg. These films are very slightly photosensitive.

It has been demonstrated that a fairly thick oxide film can be used as a protective encapsulant for these devices.

Electron microscope examination has revealed that these films are essentially continuous without defect and have a particle or grain size of less than 15 angstroms.

Preliminary experimental results have indicated that there are contaminants in the aluminum and aluminum-oxide films prepared from an alumina crucible.

### Energetic Electron Transport

The experimental program to determine the mechanisms of transport for energetic electrons through thin metal films has been carefully examined. At this time it is strongly felt that the experiment is plagued with experimental difficulties that could not be reasonably expected to be solved before the end of this contract. In addition, theoretical calculations of the problems relating to the injection, transport, and collection phenomena in the metal-base transistor have led to very low values of the terminal current transport efficiency. Thus, it is very questionable whether the results of this experiment, although of interest with regard to their material characterization implications, would be of use in the fabrication of a useful device.

## INTRODUCTION

### Aluminum-Oxide Films

The electronic properties of aluminum-oxide films prepared by reactive evaporation of aluminum in a controlled oxygen atmosphere are being determined as a function of deposition conditions. The specific deposition conditions are those of deposition rate, oxygen pressure, and surface mass. Devices are fabricated at a specific deposition rate and surface mass, and the oxygen pressure is established at a different value for a series of runs. A second experimental technique is to maintain the oxygen pressure and deposition rate at constant levels and fabricate a series of devices with incrementally varied surface mass. The analysis of the variation in capacitance per unit area with surface mass has shown that the dielectric constant and density are independent of the surface mass.

By reducing the oxygen pressure, it has been shown that the resultant oxide films may be made partially conducting. The actual resistivity obtained is critically dependent upon the oxygen pressure and the deposition rate. For the present system geometry, a critical pressure of  $6 \times 10^{-5}$  mm Hg has been determined. Films made below this oxygen pressure become semi-insulating or partially conducting, with a very rapid increase in conductivity for a small decrease in oxygen pressure. The semi-insulating films have considerably higher dielectric constant than the insulating films and, in addition, are somewhat photosensitive.

Depending upon the actual conduction mechanism in these semi-insulating films, it may be possible to fabricate field-effect active devices. Such devices could be expected to have fairly high temperature capability, since the aluminum-oxide matrix has a very high energy of formation and would not be expected to be affected by fairly high temperatures.

Aluminum was chosen for this study on the basis of previous success in fabricating aluminum oxide. Aluminum is a reasonable choice for initial experiments in reactively evaporated oxide films because of the single, stable oxide. This reduces the complexity of the experiment and should allow one to reach conclusions which could be applied to more complex systems. Magnesium exhibits similar chemical properties and would also be a reasonable choice for initial investigation. However, aluminum was chosen because of previous experience.

## Energetic Electron Transport

Fabrication of a useful metal-base transistor requires a knowledge of the injection transport and collection of the active carriers which, in this particular case, are electrons. Initial studies of the injection and collection mechanisms indicated that these mechanisms could be handled theoretically with the present knowledge regarding charge transport through and/or across energy barriers. Determination of the attenuation length of energetic electrons moving transversely through a thin metal film was not calculable without specific experimental data on the interaction mechanisms available to the carriers as they moved through the film.

In order to obtain this data, the following experiment was proposed. A specially designed low-energy electron gun was to act as a source of electrons. This electron beam was to be collected by a surface-barrier diode. The metal film under study served as the barrier contact of the diode. By measuring the fraction of the total collected current that passes through the metal film and is collected by the diode as a function of beam energy and metal film thickness, one could experimentally determine the attenuation length of the injected electrons as a function of their excess energy. Some of the problems that arise here are those of film uniformity, space-charge limitations on the beam-current density, and the necessity of reducing the work function of the collecting film in order to study the desired energy range of incident electrons.

Numerous experimental difficulties have plagued this experiment from the start and have been reported previously. In light of these problems, the entire experiment was re-evaluated and it was decided that there was little chance of obtaining useful results during the remaining time of the contract; therefore, the experimental program has been terminated.



## ALUMINUM-OXIDE FILMS

### Device Fabrication

During this reporting period a number of device runs were completed. The oxide capacitors were fabricated as indicated in the previous reports. That is, devices consisting of an aluminum electrode, an oxide layer, and an aluminum counterelectrode are deposited on a 2 x 3 cm glass substrate. Each substrate contained four small-area capacitors, four large-area capacitors, and two 4-terminal resistors. Insulating and semi-insulating oxides were prepared with varying deposition rate, oxygen pressure, and surface mass. The majority of the oxide films were prepared using an alumina crucible to contain the aluminum charge. A single oxide run was performed with a tungsten-coil evaporator.

In addition to the oxide capacitor runs, large-area oxide samples were formed on glass for X-ray diffraction, optical transmission, and electron fluorescent experiments.

Oxide samples were also fabricated on carbon-coated electron microscope grids for structural and crystallographic tests.

Large-area aluminum films for spectrographic analysis were fabricated using both the tungsten-coil and the alumina-crucible evaporator structures.

### Bulk Material Analysis

Electron microscope tests. — An insulating film of aluminum oxide 10 micrograms per cm<sup>2</sup> was deposited on a carbon-coated electron-microscope grid. These samples were then carefully installed in the microscope for electron micrographs and electron diffraction tests. As shown in Figure 1, the oxide film is continuous and without detectable defect. This is characteristic of practically the entire area of the film. There are small regions containing crystallites, but these are thought to be contamination produced during the handling. Notice that there is no discernible structure in these films.

The electron diffraction pattern, Figure 2, consists of very broad rings, which are characteristic of very small crystal size. It has been

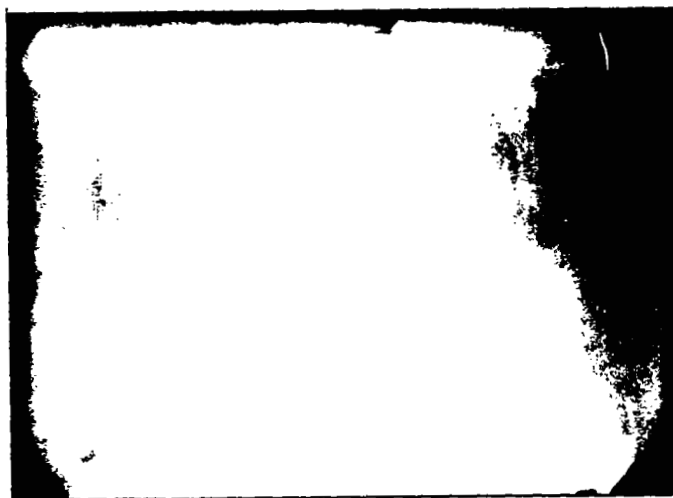


Figure 1. Electron Micrograph of Oxide Film (Dark Area), Magnification = 80,000X

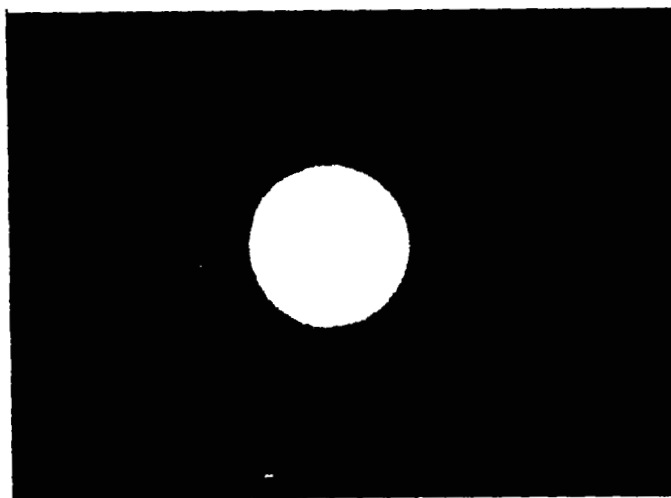


Figure 2. Electron Diffraction Pattern of Oxide Film

estimated by Mr. M. Schlacter, of the Physics and Chemistry Department, that these films are essentially amorphous, with crystallites of less than 15 angstroms.

X-ray diffraction. — A fairly thick ( $\sigma = 140$  micrograms  $\text{cm}^{-2}$ ) insulating oxide film was deposited over a 2 x 3 cm glass substrate. The X-ray diffraction pattern for the glass substrate and the oxide film showed no detectable difference. This rather coarse measurement is not in itself definitive, but when combined with the electron microscope test tends to substantiate the previous estimate of crystal size. However, the so-called thick oxide film would not be expected to have produced an appreciable X-ray diffraction unless it was highly oriented.

Electron-induced fluorescence. — A partially conducting oxide film ( $\sigma = 40$ ,  $D = 160$ ,  $P_{\text{O}_2} = 5 \times 10^{-5}$ )\* was deposited on a 2 x 3 cm glass substrate. This film was then installed in an electron-beam apparatus and attempts were made to determine whether the oxide film could be excited by the electron beam. The results of these tests were negative.

Spectrographic analysis of aluminum films. — As described in a later section of this report, there were indications of contamination of the aluminum films. In order to obtain a semiquantitative analysis of the films, thick ( $\sigma = 125$  to 300) aluminum films were deposited on a 5 x 5 cm glass substrate. Aluminum films were deposited using the alumina crucible and a tungsten-coil evaporator. These film samples, and also samples of the starting aluminum and the crucible material, have been sent to Philco's Spectrographic Laboratory, at Lansdale, for semiquantitative spectrographic analysis.

Thickness measurements. — Up to the present time, multiple-beam interferometer thickness measurements have been made on three device runs. In general, the measurements have been hampered severely by the ripples in the surface of the glass substrates which produce curved interference lines. These lines make it very difficult to obtain repeatable and accurate thickness measurements. As can be seen in Table 1, there is considerable spread in the measured thickness from device to device on the same substrate, as well as considerable spread in the thickness measured for the same device when the measurement is repeated. Because of the very large spread in the thickness data, one can only estimate a range of oxide densities, e. g.:

---

\* For the remainder of this report,  $\sigma$  has units of  $\mu\text{gm cm}^{-2}$ ;  $D$ , units of  $\text{ngm cm}^{-2} \text{sec}^{-1}$ ; and  $P_{\text{O}_2}$ , units of mm Hg.

Table 1. Oxide Thickness Measured With Multiple-Beam Interferometer

RUN NO.	DEVICE									
	1	2	3	4	Average	7	8	9	10	Average
A-15 (T in Å)	1535	1460	1500	1347	1461	1479	1450	1494	1505	1482
A-17 (T in Å)	*	*	*	*	*	1530	1552	1530	1736	1587
A-43 (T in Å)	1440	*	*	*	1440	*	1171	*	*	1171

NOTES:

1. For all the above runs, the deposition rate was  $40 \text{ ngm cm}^{-2} \text{ sec}^{-1}$ , pressure was  $2 \times 10^{-4} \text{ mm Hg}$ , and mass was  $40 \text{ } \mu\text{gm cm}^{-2}$ .
  2. Sample A-15 was a standard run.
  3. Sample A-17 was exposed to air after oxide deposition and before the last aluminum evaporation.
  4. Sample A-43 was prepared with an aluminum-coated tungsten filament.
- \* Substrate curvature produces extremely curved interference lines; no measurements were made.

$$\rho = \frac{\sigma}{T}$$

$$\sigma = 40 \text{ micrograms cm}^{-2}$$

$$T = 1170 \text{ to } 1590 \text{ angstroms}$$

$$\therefore \rho = 2.5 \text{ to } 3.4 \text{ grams cm}^{-3}$$

The large spread in thickness values does not correlate with the capacity measurements which produced essentially constant capacitance per unit area for all these devices.

Additional multiple-beam interferometer thickness measurements will be made on optically polished quartz resonator crystals that will be installed in the vacuum system as the sensing element for a second resonant quartz microscale. By using this technique, mass per unit area and thickness measurements will be performed on the same sample. This will eliminate any error that might be caused by source distribution. It is hoped that the optically polished crystal will have both long- and short-range flatness, which will eliminate the curved interference lines. By using this technique, we should be able to determine the density and thickness to better than 5 percent.

### Electronic Device Evaluation

Effects of varying O<sub>2</sub> pressure. — A sufficient number of devices have been fabricated at varying oxygen pressure so that one can now attempt to describe the variation in oxide properties with oxygen pressure. Oxide films were prepared at a constant deposition rate of 160 and a constant surface mass of 40. Oxygen pressure was then varied for each run from  $2 \times 10^{-4}$  down to  $4.8 \times 10^{-5}$ . The results of this experiment are summarized in Figures 3 to 6, which are plots of the capacitance per unit area, dissipation factor,  $\rho_f \epsilon_r$  product, and the ac resistance as a function of oxygen pressure. All of this data was obtained at a frequency of  $10^5$  cps. For all the parameters measured, the variation in oxygen pressure produced small and nearly negligible results as long as the minimum critical pressure was maintained. If the oxygen pressure was reduced to below the critical pressure of approximately  $6 \times 10^{-5}$ , there was a drastic increase in the admittance of the film. Both the ac conductance and the capacitance increased drastically for oxygen pressures below the critical pressure.

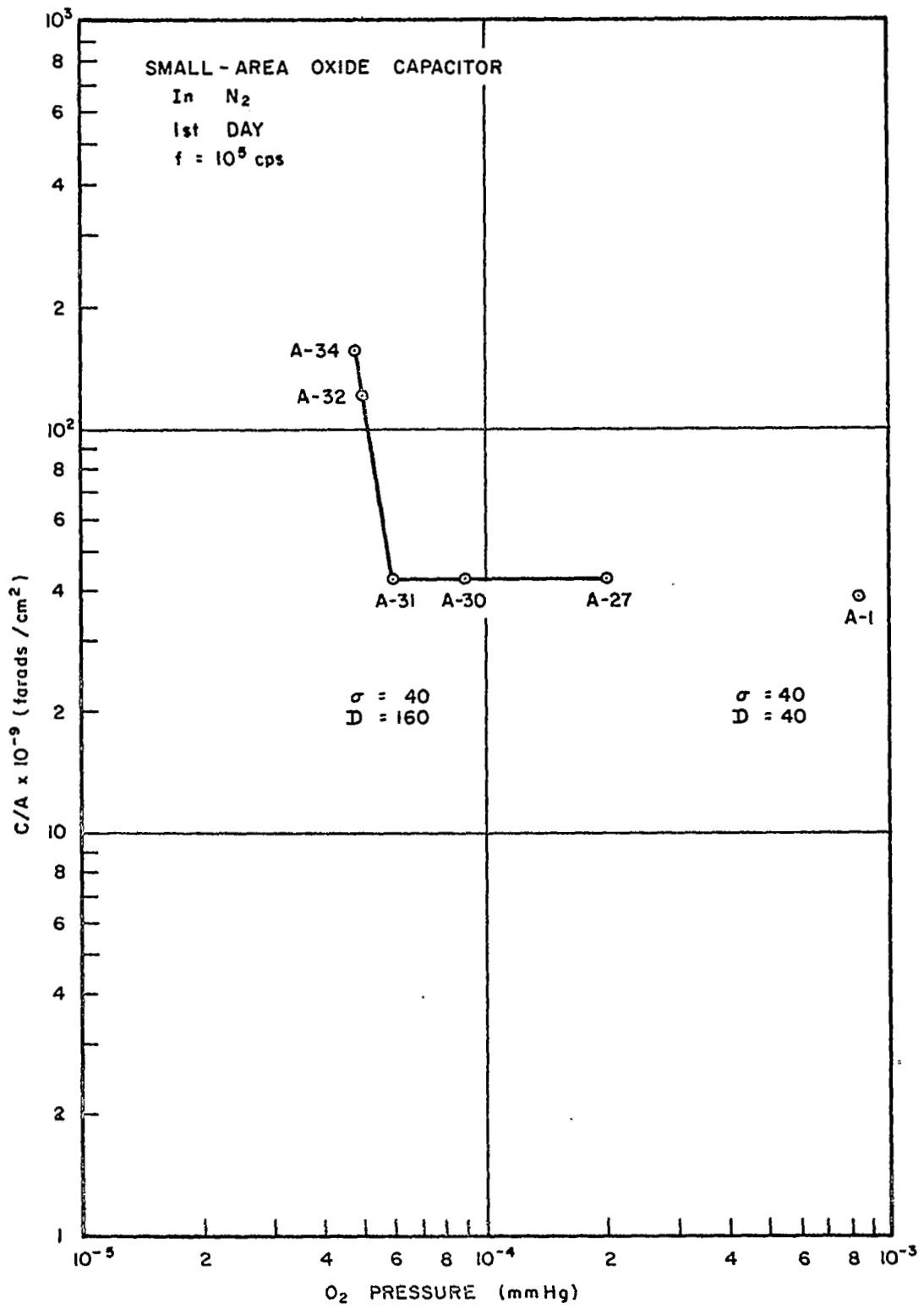


Figure 3. C/A Versus O<sub>2</sub> Pressure

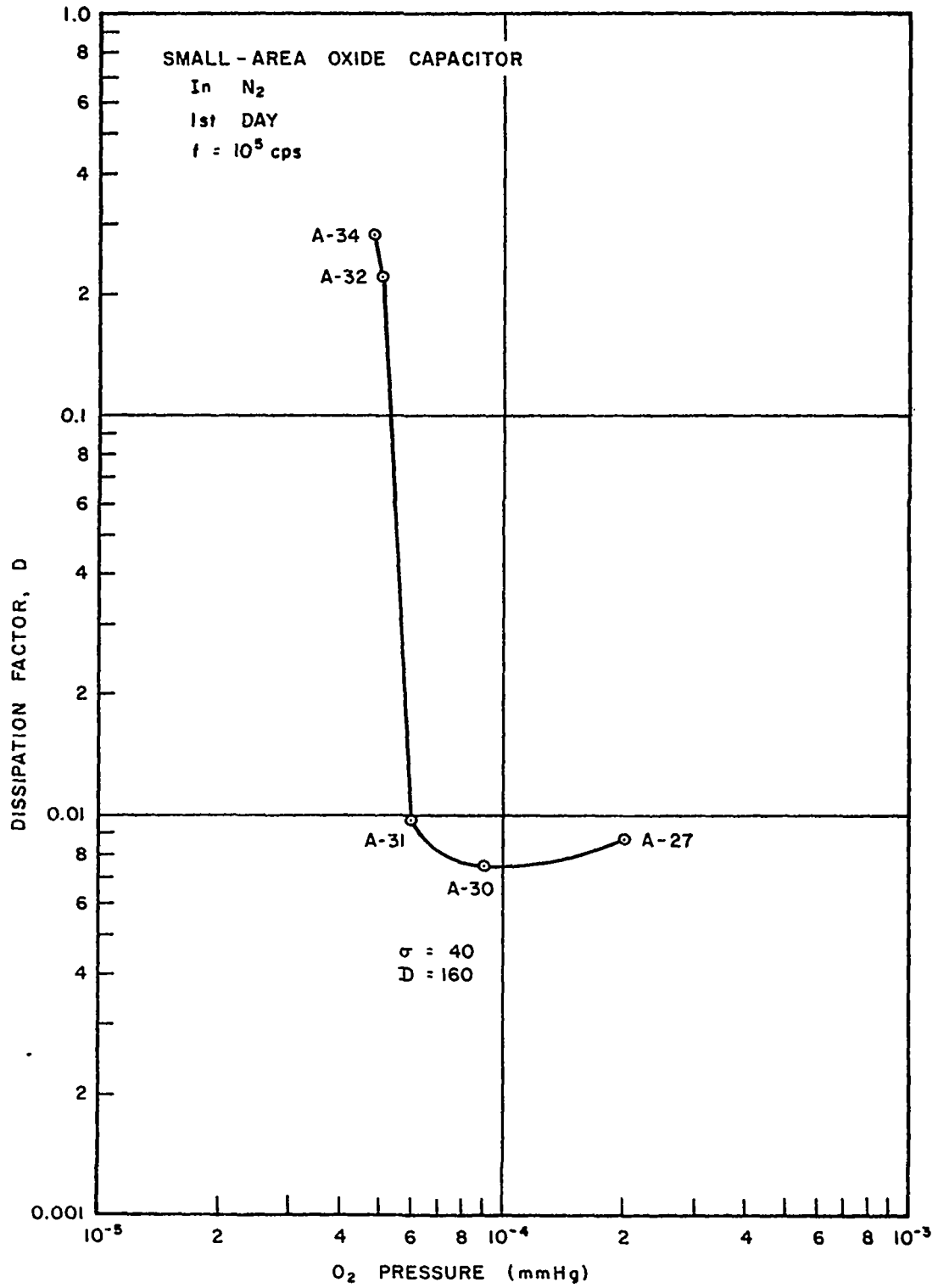


Figure 4. Dissipation Factor Versus O<sub>2</sub> Pressure

FOR OXIDE CAPACITOR

In N<sub>2</sub>

1st DAY

f = 10<sup>5</sup> cps

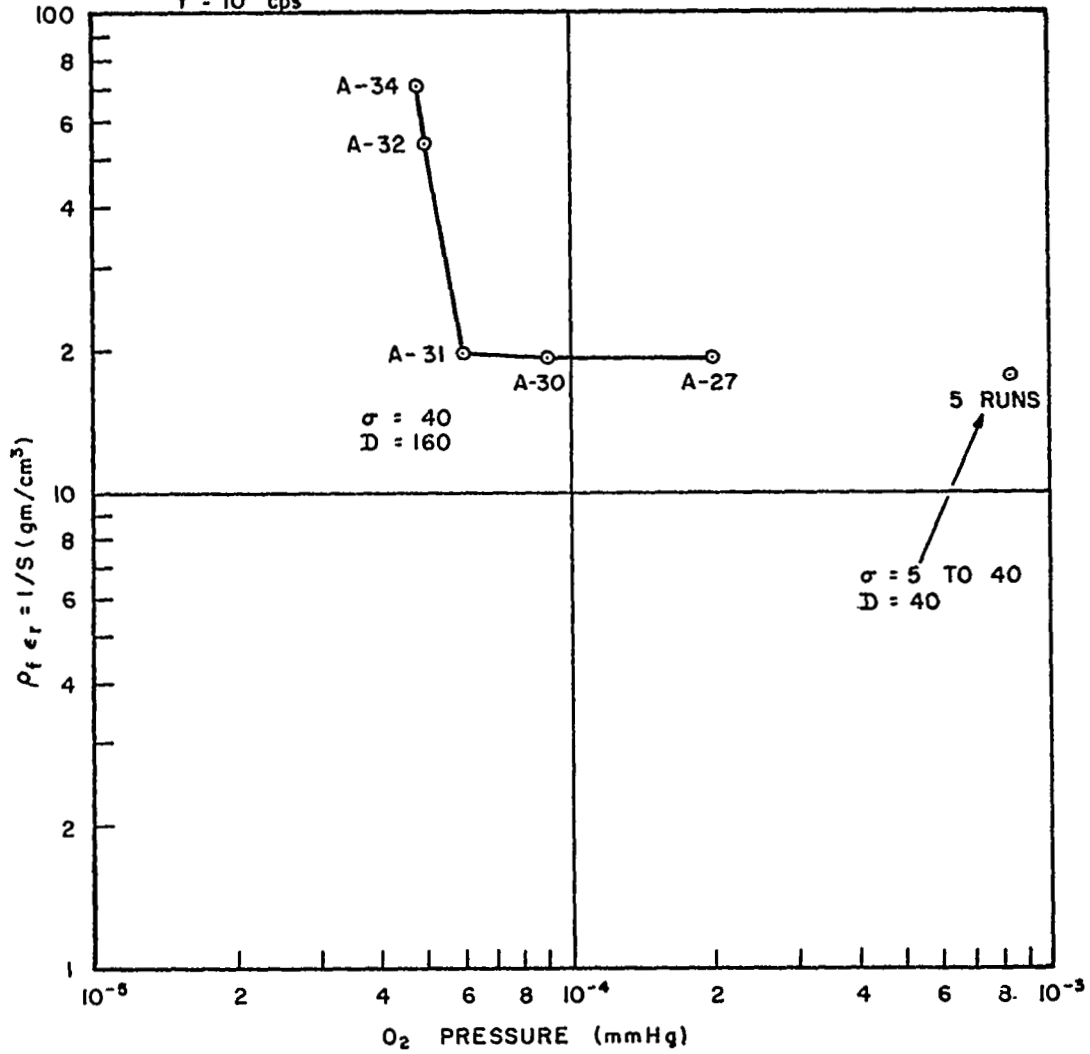


Figure 5.  $\rho_f \epsilon_r$  Versus  $O_2$  Pressure



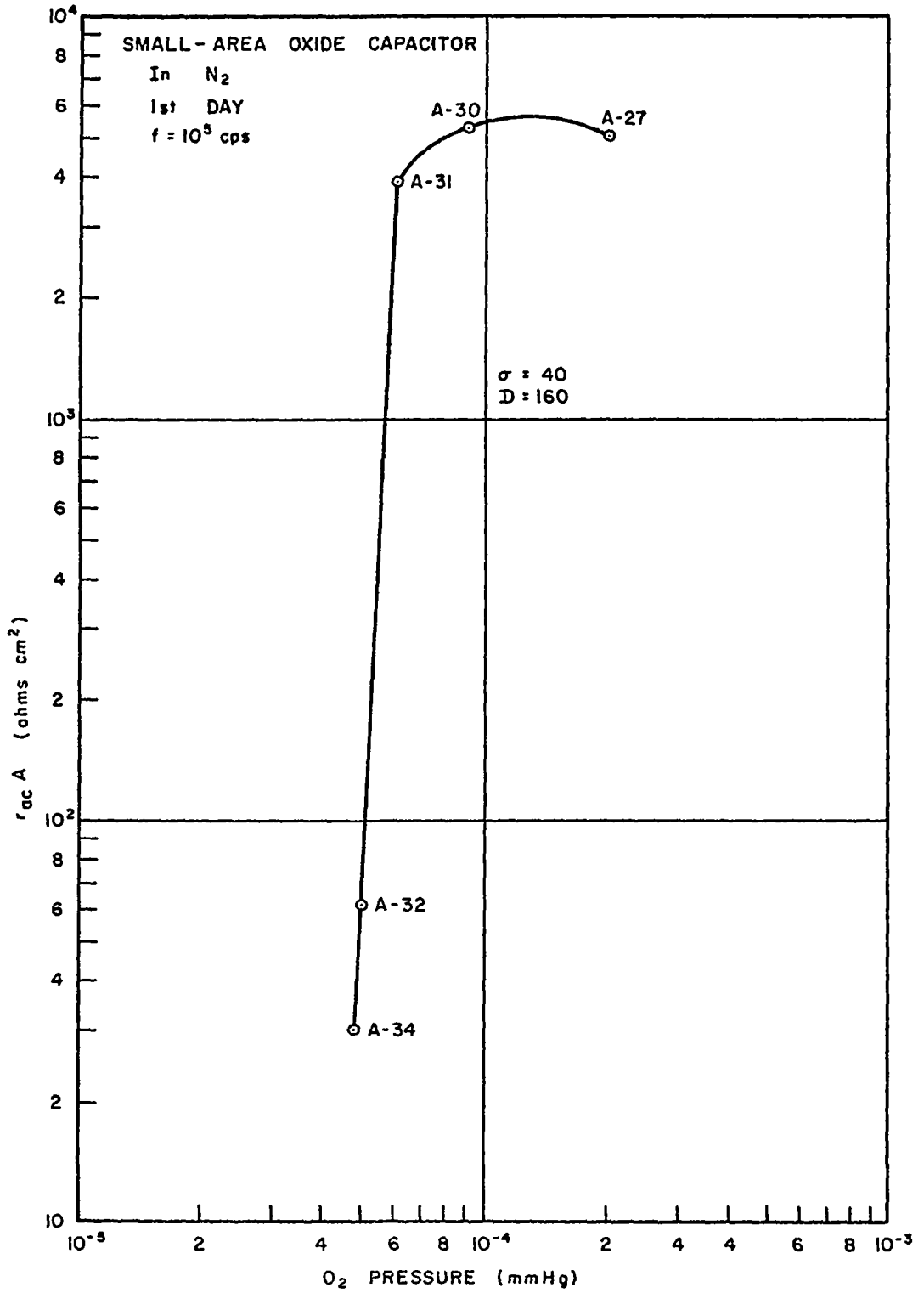


Figure 6.  $r_{ac}$  Versus O<sub>2</sub> Pressure

Only the dissipation factor had an optimum value of oxygen pressure; that is, a minimum in the dissipation factor was found for oxygen pressures in the vicinity of  $9 \times 10^{-5}$ .

This result can be reasonably explained in the following manner. As long as the oxygen pressure is sufficiently high, all of the aluminum will react and form an insulating oxide. However, if the oxygen pressure is reduced, the probability of an aluminum atom not being oxidized increases. It is expected that a low concentration of free aluminum in the oxide film may provide free carriers and thus substantially increase the conductivity in the same manner that conventional doping does in a semiconductor, where the addition of a small amount of impurity can drastically influence the conductivity. With a knowledge of the oxygen pressure and the mass deposition rate of the composite film, one can calculate that the limiting pressure at which there is just enough oxygen available to totally oxidize the aluminum film is  $6 \times 10^{-5}$  for a deposition rate of 40. The experimental data shows that the actual critical pressure is substantially higher than this, which seems to indicate that the excess aluminum is actually providing free carriers for conduction in the oxide film.

Depending upon the mode of conduction in the semi-insulating films produced at oxygen pressures below the critical pressure, it may be possible to modulate the conductivity by a transverse field and thus produce a field-effect transistor device. Experimentally, a very small (approximately 0.1 percent) photo conductivity has been observed. Further evaluation of the semi-insulating films is necessary to determine the conduction mechanism and the feasibility of constructing active devices.

Effects of ambient gas. — As reported previously, the capacitance and conductances of metal-oxide-metal sandwiches increase substantially as the units are aged in nitrogen. When the devices are exposed to air there is a steep increase in capacity and conductance. After considerable aging, samples exposed to air display a decrease in capacity and conductance. The thinner samples show substantially smaller percentage variations. In addition, the transient change upon exposure to air is considerably reduced by storing the devices in dry nitrogen for an extended period of time (30 days).

To eliminate the effects of ambient, the devices fabricated on run A-28 were overcoated with a thick oxide layer,  $\sigma = 300$ . The results of the capacitance and resistance measurements made at  $10^5$  cps on the oxide

passivated sample and two unpassivated samples are summarized in Figures 7 and 8. Note that the initial capacitance for runs A-27 and A-28 is substantially larger than for run A-1. This has been experimentally determined to be due to the variation in deposition rate. Runs A-27 and A-28 were fabricated at a deposition rate of 160, whereas run A-1 was fabricated at a deposition rate of 40. The oxide passivated unit had a small initial increase in capacitance during the first day, but showed negligible capacitance change during the following 30-day period. Devices from runs A-1 and A-27 exhibited similar increase in capacitance during their storage in nitrogen gas. However, run A-1 was exposed to air after 3 days of nitrogen storage. This action resulted in a steep increase in capacitance, followed by a long time decrease which is extending over a period of at least 70 days.

A similar examination of Figure 8 reveals the substantial reduction in the variation of the ac shunt resistance for the passivated unit. Although these preliminary results are by no means conclusive, it does appear that a fairly thin oxide film can provide a considerable improvement in the stability of the device electrical characteristics. An investigation of the degree of protection as a function of oxide thickness is planned.

Film contamination. — Admittance frequency curves have been obtained on a number of device samples over the frequency range from  $10^2$  to  $10^5$  cps. In general, the minimum dissipation factor of 0.01 is obtained at a frequency of 100 kc. The capacitance of these samples is essentially independent of frequency. In a dielectric where the internal loss mechanism is due to a resonance which occurs at a frequency much higher than the measuring frequency, one could expect that the dissipation factor of the dielectric would be independent of frequency, at least down to fairly low frequencies where a parallel leakage resistance will increase the dissipation factor. The results of our initial impedance-frequency measurements have indicated that the dissipation factor has a minimum at about 10 kc and increases on all samples to approximately 0.01 at 100 kc. This increase in dissipation factor is easily explained if one has a suitably large series resistance. For oxide films of  $40 \text{ micrograms cm}^{-2}$ , a series resistance of 15 ohms is required for the small-area devices and 3 ohms for the large-area units. This amount of series resistance is much larger than one can expect for the electrodes. A calculation of the electrode resistance indicated that the small sample should have approximately 3 ohms of series resistance, but measurement of the actual electrodes indicated a series resistances of 14 ohms. Although the measured series resistance is sufficient to explain the dissipation-factor increase seen at  $10^5$  cps, it was

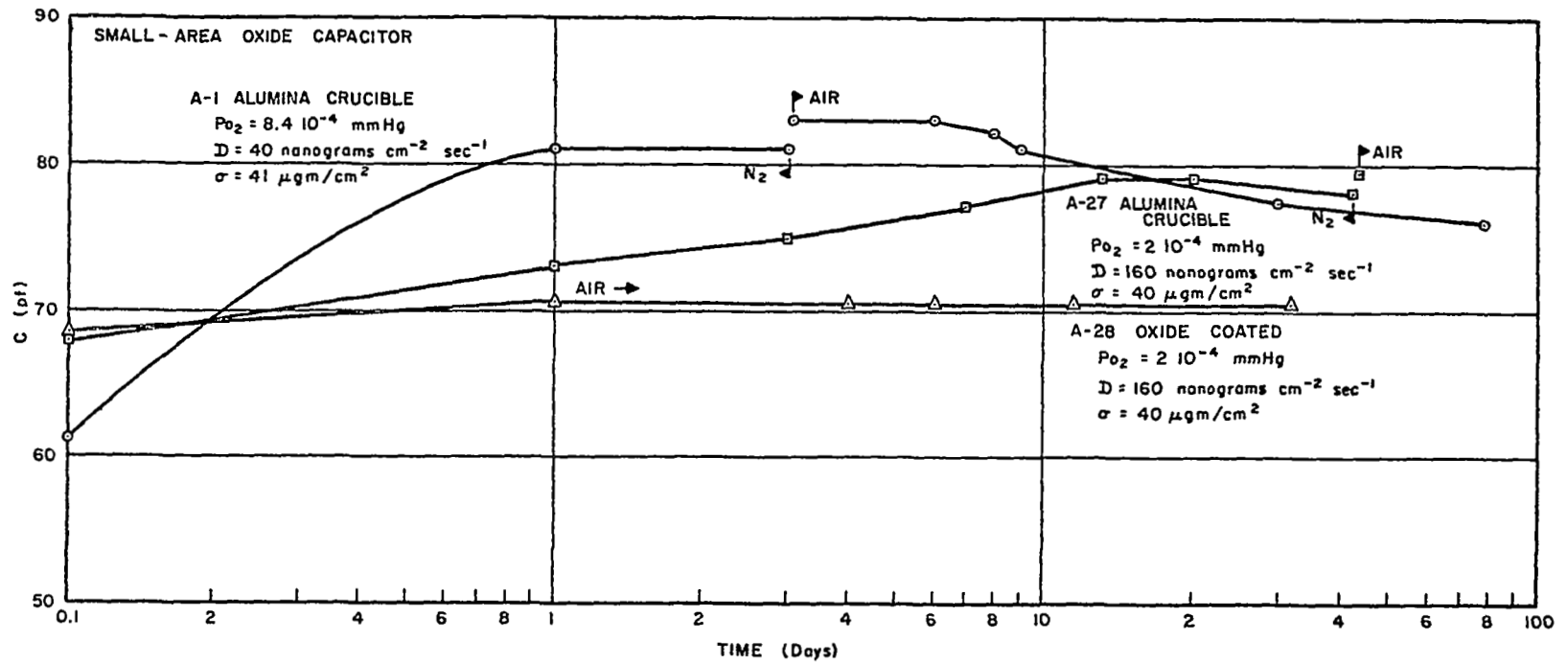
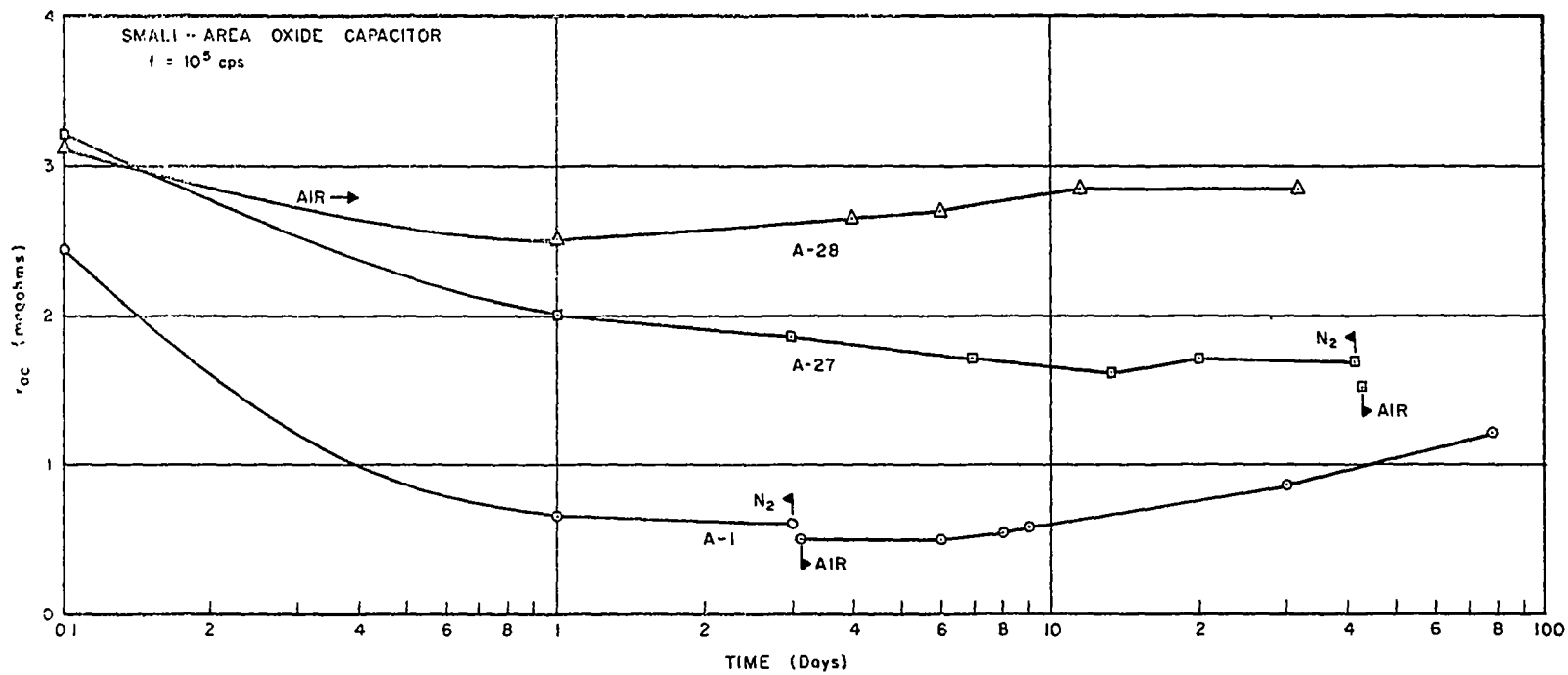


Figure 7. Capacity Versus Time

Figure 8.  $r_{ac}$  Versus Time

still much larger than expected. For this reason the evaporation technique was examined to determine whether there were contaminants in the films which could produce this increase in resistance.

While determining the effects of the deposition technique on the oxide dissipation factor, it was found that there is a large spurious coupling between the signal source and the internal detector in the General Radio 1650-A bridge which produces very large errors in dissipation factor if the internal level control is used to attenuate the signal applied to the device under test. In addition, the inherent accuracy of the bridge at 10 kc is very poor for dissipation factors of 0.01 or less. The error due to the spurious internal coupling can be eliminated by using an external oscillator and level control, which allows one to set the internal level control at full on. By using the 1650-A bridge in this manner and combining these results with data obtained at  $10^5$  and  $10^6$  cycles per second obtained from precision Pointon capacitance bridges, the dissipation factor as a function of frequency was obtained for devices in runs A-27, A-43, and A-28. The results of these tests are summarized in Figure 9. The capacitance of these samples was essentially dependent of frequency as shown in Figure 10.

The following tentative conclusions may be derived from an examination of the variation of dissipation factor with frequency. First, the high-frequency loss in runs A-27 and A-28, which were made using an alumina crucible, is increased by the series resistance of the metal electrodes. Run A-43, which was prepared using a tungsten-coil evaporator for the entire run, shows a much smaller increase in dissipation factor at 1.0 megacycle, which is to be expected since the series resistance of the metal films has been reduced by approximately five to one.

In the middle- and low-frequency region, differences in dissipation factor tentatively can be explained as follows. Run A-27, which was not oxide coated and prepared with the alumina crucible, could contain impurities in the oxide film; when exposed to atmosphere, the impurities produce mobile ions which, at low frequencies, could follow the applied field and thereby increase the dissipation factor. Device run A-43, however, was prepared using a tungsten-coil evaporator and may therefore not contain the same contaminants. Thus, exposure to atmosphere results in a smaller ionic current and therefore a lower dissipation factor. The lowest dissipation factor of all was obtained on run A-28. The devices in run A-28 were fabricated using an alumina crucible and were then overcoated with a thick oxide protective layer. These devices would be expected to contain impurities similar to those in run A-27. However, the oxide passivation

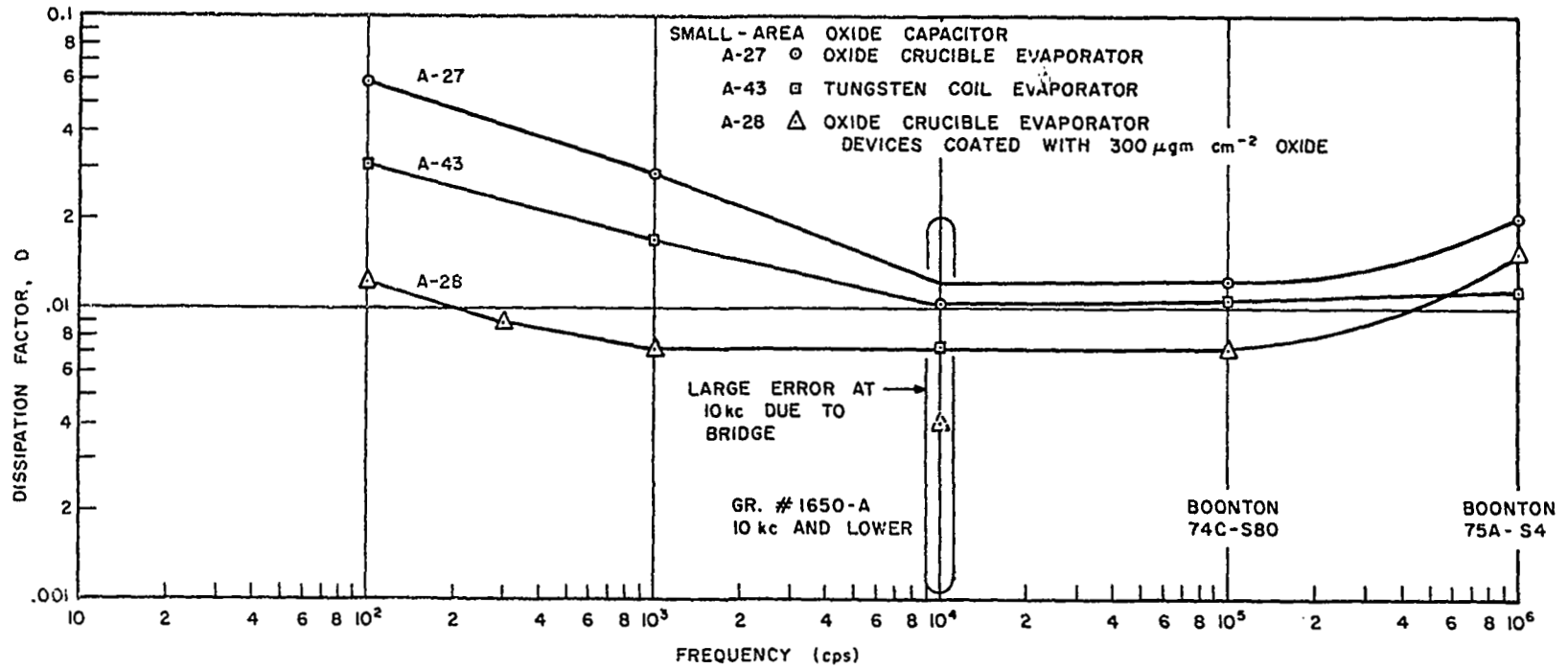


Figure 9. Dissipation Factor Versus Frequency

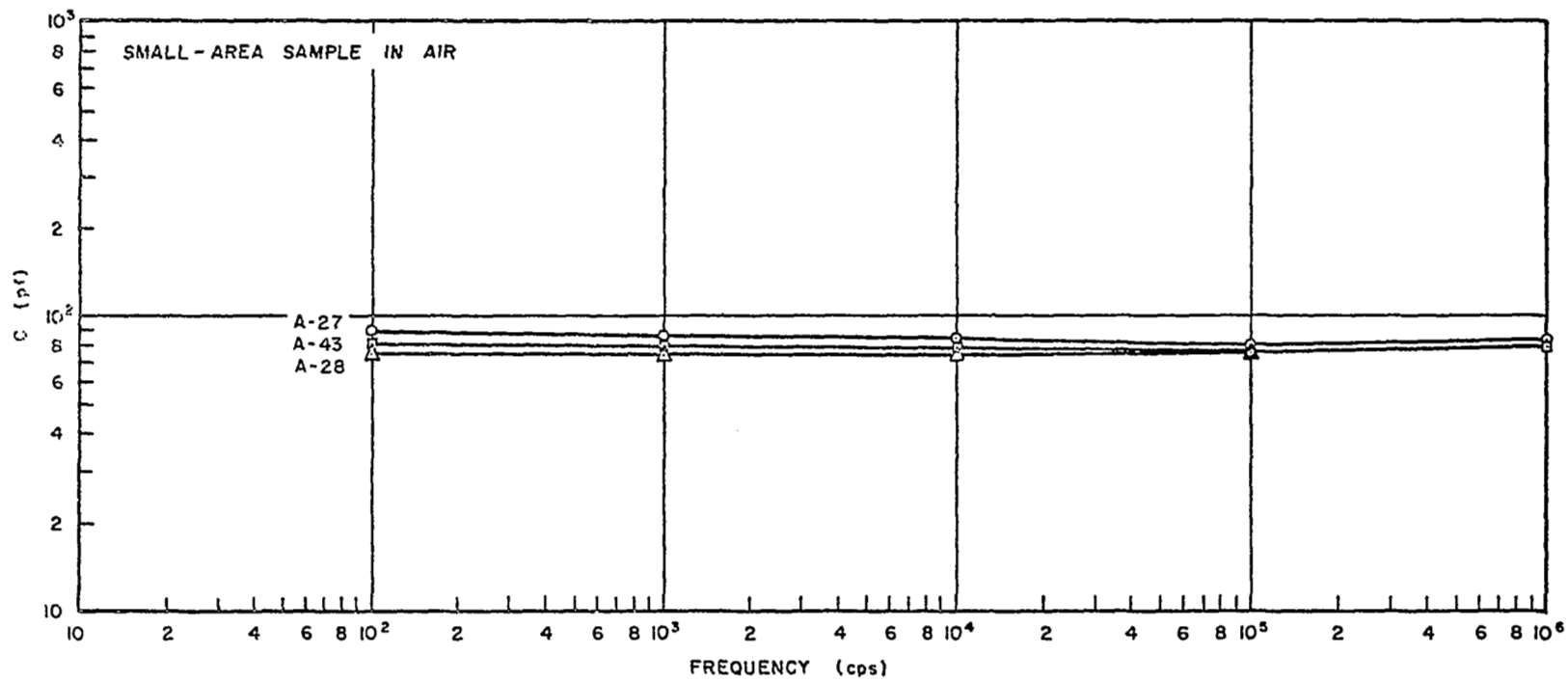


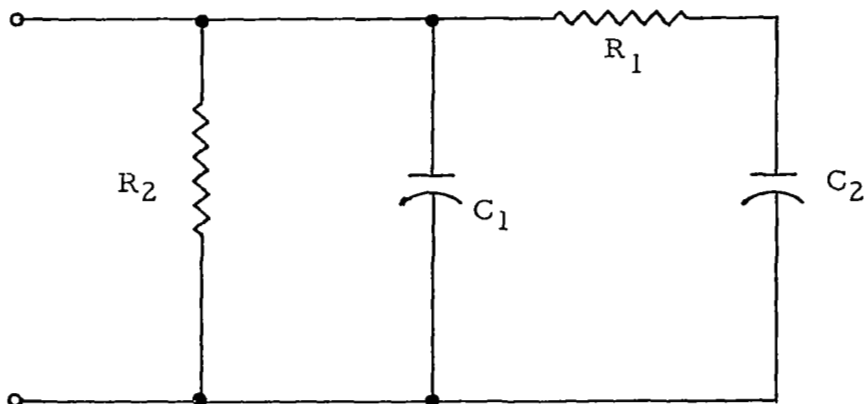
Figure 10. Capacitance Versus Frequency



prevents the atmospheric diffusion into the sample and thereby does not allow the entrapped impurities to become free ions; thus, the decrease in dissipation factor as compared to run A-27.

This explanation is not intended to be final, but may be considered a tentative and reasonable one. Further experiments with devices similar to those in run A-43, but with an oxide protective layer, will be fabricated. These devices should have a dissipation factor measurably smaller than any of those made before.

DC I-V characteristics. — Attempts to measure the dc I-V characteristics of thin samples were frustrated by a very large hysteresis effect that definitely was not associated with the geometrical capacitance. Further investigation of this anomalous effect indicated that an equivalent circuit similar to that shown below would explain the hysteresis in the I-V characteristic as well as the long time required before the  $R_{dc}$  value would stabilize.



In this equivalent circuit,  $C_1$  represents the geometrical or high-frequency capacitance, and  $R_1$  is high-frequency loss. These are the parameters that one would measure at 100 kc if the effects of series resistance loss could be neglected.  $R_2$  represents the dc leakage through the oxide film, and  $C_2$  is a mysterious capacitance whose value is of the order of 10 to 100 times that of  $C_1$ . The nature of this capacitance is not at all clear at this time. Conceivably, charge trapping or ion migration in the oxide could account for this capacitance. It should be noted that  $R_1$  can be frequency sensitive.

Although quantitative tests have not been completed, preliminary results have indicated that there is a strong correlation between the hysteresis

in the I-V characteristic and the low-frequency dissipation factor. As mentioned previously, there appears to be a correlation between the contaminants in the film and atmospheric exposure with the low-frequency dissipation factor. It has also been found that the time constant associated with  $R_1 C_2$  is correlated with the fabrication techniques in the same manner as the dissipation factor. That is to say, devices which exhibit the highest dissipation also have the largest hysteresis in their I-V characteristics. It is also interesting to note (Figure 10) that although the high-frequency capacitances of the three device runs were essentially identical, the device run with the largest low-frequency dissipation factor exhibited a significant increase in capacitance with decreasing frequency. All the previously discussed variations in dissipation factor, capacitance, and I-V hysteresis are tentatively explained if one allows mobile ions to occur in the oxide film.

### Conclusions

The electrical properties of oxide films have been shown to be dependent on the oxygen pressure and deposition rate. By reducing the oxygen pressure below a critical value ( $6 \times 10^{-5}$ ) the resulting film exhibits a photosensitive conductivity. In addition, these aluminum-oxide films have a higher dielectric constant and dissipation factor than the insulating films.

Insulating films have been studied with the electron microscope and were determined to be essentially amorphous with a grain size of less than 15 angstroms.

The sensitivity of these devices to atmospheric exposure is substantially reduced by overcoating the active device area with a thick reactively deposited oxide film.

Although the data is not yet complete, it appears that a combination of impurities from the alumina crucible and the exposure to room air result in an increase in dissipation factor and that this increase is related to the hysteresis in the I-V characteristic.

## ELECTRON TRANSPORT THROUGH THIN FILMS

### Transport Experiment

During the early phases of this program, an experiment was being developed from which to obtain further information on processes affecting the collection of hot electrons at a metal semiconductor barrier. This experiment was designed to check theoretical predictions made concerning this collection process under a previous contract (DA-36-039-SC-90715). A complete description of the experimental details is contained in the first quarterly report issued under the present contract. While attempting to develop this experiment, difficulties were encountered in achieving the low-energy electron gun and the large-area metal semiconductor barrier. These difficulties, discussed in previous quarterlies, delayed substantially the planned rate of progress and led to a re-evaluation of the justification for and the necessity of continuing the experiment. From this re-evaluation came the conclusion that, although the information which might be gained from such an experiment could conceivably shed much light on basic hot-electron phenomena such as transport and collection, it was unlikely that it would change the conclusion (based on theoretical grounds) that hot-electron-effect triodes would not likely be useful for circuit applications.

In summary, it can be said that metal-insulator versions of the hot-electron triode, e. g. , the tunnel-emitter version suggested by Mead, will of necessity, be limited in current gain by factors such as back scattering on electrons out of the collector barrier interface and low-angle electron phonon scattering in the metal base layer. The arguments in support of this prediction of low current gain are so convincing and difficulties anticipated in obtaining of their experimental confirmation were so discouraging that it was decided the research effort to be spent in this portion of the program would most profitably be utilized in achieving better control over the film materials needed for successful device development. For this reason, the experiment on electron transport was discontinued at the midpoint of this program.

## Conclusions

Due to extensive experimental problems with the electron gun and the collector diode, the probability of success in obtaining data in the mean-free-path of hot electrons during the remainder of this contract is very doubtful. In addition to this, theoretical calculations of the terminal current gain of a hot-electron triode have indicated that there is very little chance of making a useful device. For these reasons the energetic electron transport experiment has been terminated.

## OVERALL CONCLUSIONS

### Aluminum-Oxide Films

It has been determined experimentally that the metal films and possibly the oxide films deposited from the alumina crucible contain a sufficient amount of impurity to alter their electrical characteristics. Devices fabricated using a tungsten-coil evaporator have shown significant improvement in both the oxide- and metal-film electrical properties. The metal films have a resistivity equivalent to that of bulk material and the oxide films have significantly lower dissipation factors when deposited using the tungsten coil.

The dielectric properties of the oxide film vary systematically with the oxygen pressure; that is, a reduction in the oxygen pressure results in a systematic increase in the dielectric constant, the dissipation factor, and the conductivity of the oxide for oxygen pressures below a critical value. Semi-insulating oxide films exhibit a slight photosensitivity.

DC measurements of the oxide films have been severely hampered by very slow processes which may be trapping and/or ion movement in the oxide film.

The oxide films exhibit variations in capacitance and dissipation factor dependent upon the storage ambient. These effects can be essentially eliminated by coating the device with a fairly thick ( $\sigma = 130$ ) oxide film. Exposure to atmosphere of protected devices does not result in any detectable electrical parameter variations.

Preliminary measurements of thickness have yielded a density of 2.5 to 3.4 grams per cubic cm for the oxide films as compared to approximately 4 grams per cubic cm for sapphire.

### Energetic Electron Transport

The status of the energetic electron transport experiment has been carefully reviewed; because of the number of experimental problems and the difficulty of overcoming these problems, the experiment has been terminated.